

# Extracellular phosphorylation of the amyloid $\beta$ -peptide promotes formation of toxic aggregates during the pathogenesis of Alzheimer's disease

Sathish Kumar<sup>1</sup>, Nasrollah Rezaei-Ghaleh<sup>2</sup>,  
Dick Terwel<sup>1</sup>, Dietmar R Thal<sup>3</sup>,  
Mélisande Richard<sup>4</sup>, Michael Hoch<sup>4</sup>,  
Jessica M Mc Donald<sup>5</sup>, Ullrich Wüllner<sup>1</sup>,  
Konstantin Glebov<sup>1</sup>, Michael T Heneka<sup>1</sup>,  
Dominic M Walsh<sup>5</sup>, Markus Zweckstetter<sup>2,6</sup>  
and Jochen Walter<sup>1,\*</sup>

<sup>1</sup>Department of Neurology, University of Bonn, Bonn, Germany,

<sup>2</sup>Department for NMR-based Structural Biology, Max-Planck-Institute for Biophysical Chemistry, Göttingen, Germany, <sup>3</sup>Department of Pathology, University of Ulm, Ulm, Germany, <sup>4</sup>Department of Molecular Developmental Biology, LIMES Institute, University of Bonn, Bonn, Germany, <sup>5</sup>Laboratory for Neurodegenerative Research, University College Dublin, Dublin 4, Ireland and <sup>6</sup>DFG Research Center for the Molecular Physiology of the Brain (CMPB), Göttingen, Germany

**Alzheimer's disease (AD) is the most common form of dementia and associated with progressive deposition of amyloid  $\beta$ -peptides (A $\beta$ ) in the brain. A $\beta$  derives by sequential proteolytic processing of the amyloid precursor protein by  $\beta$ - and  $\gamma$ -secretases. Rare mutations that lead to amino-acid substitutions within or close to the A $\beta$  domain promote the formation of neurotoxic A $\beta$  assemblies and can cause early-onset AD. However, mechanisms that increase the aggregation of wild-type A $\beta$  and cause the much more common sporadic forms of AD are largely unknown. Here, we show that extracellular A $\beta$  undergoes phosphorylation by protein kinases at the cell surface and in cerebrospinal fluid of the human brain. Phosphorylation of serine residue 8 promotes formation of oligomeric A $\beta$  assemblies that represent nuclei for fibrillization. Phosphorylated A $\beta$  was detected in the brains of transgenic mice and human AD brains and showed increased toxicity in *Drosophila* models as compared with non-phosphorylated A $\beta$ . Phosphorylation of A $\beta$  could represent an important molecular mechanism in the pathogenesis of the most common sporadic form of AD.**

*The EMBO Journal* (2011) 30, 2255–2265. doi:10.1038/emboj.2011.138; Published online 28 April 2011

**Subject Categories:** neuroscience; molecular biology of disease

**Keywords:** Alzheimer's disease; amyloid  $\beta$ ; oligomers; post-translational modification; protein folding

\*Corresponding author. Department of Neurology, University of Bonn, Molecular Cell Biology, Sigmund-Freud-Strasse 25, 53127 Bonn, Germany. Tel.: +49 228 287 19782; Fax: +49 228 287 14387; E-mail: Jochen.Walter@ukb.uni-bonn.de

Received: 19 October 2010; accepted: 4 April 2011; published online: 28 April 2011

## Introduction

The post-translational modification by phosphorylation has an important role in the regulation of protein activity. Protein kinases that catalyse the phosphorylation reaction mainly exert their activity towards intracellular targets and thereby regulate important physiological and pathophysiological processes, including cellular metabolism, differentiation and proliferation. In addition to intracellular protein kinases, several kinase activities have been demonstrated at the cell surface and in extracellular fluids (Chen *et al*, 1996; Redegeld *et al*, 1999). These ecto-protein kinases phosphorylate cell surface localized as well as extracellular soluble proteins, including proteins of the complement system, coagulation factors and cell adhesion proteins. Several distinct ecto-protein kinases have been characterized and appear to be very similar to intracellular kinases, such as protein kinases (PK) A, C, CK1 and CK2 (Kübler *et al*, 1989; Walter *et al*, 1996). However, the physiological and/or pathophysiological significance of extracellular protein phosphorylation is poorly understood.

Alzheimer's disease (AD) is the most common form of dementia and associated with the progressive accumulation of amyloid  $\beta$ -peptides (A $\beta$ ) in form of extracellular amyloid plaques in the human brain. A $\beta$  derives from the amyloid precursor protein (APP) by proteolytic processing. The sequential cleavage of APP by enzymes called  $\beta$ - and  $\gamma$ -secretase leads to secretion of A $\beta$  from cells into extracellular fluids (Selkoe, 2001; Mattson, 2004). A $\beta$  peptides could aggregate and form insoluble fibrils that represent major components of extracellular plaques. The role of plaque deposition in the pathogenesis of AD and particularly their neurotoxic properties are currently under debate. However, a close relationship of plaques and impaired dendritic activity supports the critical role of plaques in neurotoxicity (Spires-Jones *et al*, 2007; Koffie *et al*, 2009; Meyer-Luehmann *et al*, 2009). Notably, recent research also strongly supports an important role of small oligomeric forms of A $\beta$  in neurotoxicity and degeneration (Yankner, 1996; Chiti and Dobson, 2006; Haass and Selkoe, 2007; Selkoe, 2008).

A critical role of A $\beta$  in the pathogenesis of AD is strongly supported by gene mutations that cause early-onset familial forms of the disease. Such mutations have been identified in the APP gene itself and in presenilin 1 and 2. Importantly, all mutations identified in the different genes commonly lead to early deposition of extracellular plaques likely by increasing the generation and/or aggregation of A $\beta$  (Nilsberth *et al*, 2001; Kennedy *et al*, 2003; Tanzi and Bertram, 2005; Hori *et al*, 2007; Di *et al*, 2009).

The aggregation of A $\beta$  and other proteins that cause neurodegenerative and other diseases appears to follow similar pathways and depends on the formation of small soluble nuclei that could act as seeds and thereby promote rapid fibril growth (Harper and Lansbury, 1997; Soto and

Estrada, 2008). Thus, the assembly of monomeric proteins or peptides into smaller oligomeric structures is the rate-limiting step in fibril formation. Certain mutations within the A $\beta$  domain that cause early-onset AD (EOAD) promote formation of oligomeric assemblies and fibrillization (Kirkitadze *et al*, 2001; Murakami *et al*, 2003; Tomiyama *et al*, 2010). However, such disease causing mutations in the A $\beta$  domain are very rare and only account for a few cases of EOAD.

Mechanisms that drive formation of oligomeric nuclei of wild-type (WT) A $\beta$  and thereby might promote the pathogenesis of AD remain largely unclear. However, studies on pyroglutamate-modified variants of A $\beta$  suggest a critical role of N-terminal modification in the aggregation process (Schilling *et al*, 2008). Whether other post-translational modifications could affect A $\beta$  deposition is unknown. Here, we sought to determine whether extracellular A $\beta$  could be phosphorylated by ecto-protein kinase in the brain and its pathophysiological implications.

## Results

### Phosphorylation of extracellular A $\beta$ by ecto-PKA

To test the phosphorylation of extracellular A $\beta$ , primary cultures of mouse cortical neurons were incubated with synthetic A $\beta$  and [ $\gamma$ - $^{32}$ P]ATP. A $\beta$  was readily phosphorylated (Figure 1A). No radiolabelling was observed in the absence of cells (data not shown), indicating the presence of an ecto-protein kinase at the surface of neurons that phosphorylates A $\beta$  (Figure 1A). A $\beta$  was not detected in the corresponding cell lysates, suggesting that A $\beta$  was not internalized and phosphorylated by intracellular kinases under the experimental conditions (Figure 1B). *In silico* analysis revealed serine residue 8 (Ser8) within a potential recognition motif (R-x-x-S) for PKA (Figure 1C). Phosphorylation of extracellular A $\beta$  was significantly reduced in the presence of the selective PKA inhibitor H-89, indeed indicating an involvement of an extracellular PKA activity. However, cAMP did not further stimulate A $\beta$  phosphorylation (Figure 1D and E). These findings are consistent with a selective secretion of PKA catalytic subunits and the absence of extracellular regulatory  $\beta$ -subunits that has been demonstrated previously in tumour cells (Cho *et al*, 2000b).

To directly demonstrate phosphorylation of A $\beta$  by PKA, different variants of A $\beta$  were incubated with purified PKA *in vitro*. PKA readily phosphorylated A $\beta$ 40 or A $\beta$ 42, the two major variants in the human brain. Further *in vitro* assays using truncated variants, including A $\beta$ 1-16, A $\beta$ 17-40 and pre-phosphorylated A $\beta$  variants, confirmed the selective phosphorylation of A $\beta$  by PKA at Ser8 (Figure 1F, G and H; Supplementary Figure S1A and B). Phosphorylation of A $\beta$  was detected at low nanomolar concentrations of ATP (Supplementary Figure S1C and D), indicating that physiological concentrations of extracellular ATP in biological fluids allow phosphorylation of A $\beta$  *in vivo*.

To assess the presence of extracellular PKA activity in the human brain, we performed *ex vivo* phosphorylation assays with human cerebrospinal fluid (CSF). CSF was incubated with [ $\gamma$ - $^{32}$ P]ATP and histone, a cognate substrate for PKA. Notably, histone was efficiently phosphorylated by endogenous kinase activity in the CSF. Since this phosphorylation was strongly reduced by H-89, these data confirm the presence of an extracellular PKA-like activity in human CSF (Figure 1I).

Importantly, human CSF also contained A $\beta$  phosphorylating activity that could be efficiently inhibited by several PKA-specific inhibitors (KT5720, PKI and H-89) or by immunodepletion of PKA (Figure 1J). These combined data demonstrate the presence of extracellular PKA in the human brain that could phosphorylate A $\beta$  at Ser8.

### Phosphorylation of A $\beta$ promotes its aggregation

We next assessed whether the phosphorylation of Ser8 affects the aggregation of A $\beta$ . Phosphorylated A $\beta$  (pA $\beta$ ) and non-phosphorylated A $\beta$  (npA $\beta$ ) were incubated and aggregation was monitored by Thioflavin T (Figure 2A) or Congo Red assays (Supplementary Figure S2). npA $\beta$  showed the expected behaviour in aggregation with a pronounced lag phase before rapid fibril growth in both assays (Figure 2A; Supplementary Figure S2). Notably, pA $\beta$  showed significantly increased aggregation as compared with npA $\beta$ . However, both variants formed characteristic fibrils highly similar in morphology and size at the end point of this assay (Figure 2B). The analysis of aggregation kinetics revealed that npA $\beta$  takes about five times longer to exit the lag phase than pA $\beta$  (Supplementary Table S1). It is also interesting to note that, despite the remarkably faster aggregation of pA $\beta$  than npA $\beta$ , their apparent rate constant values ' $k$ ' were very similar. Altogether, these data suggest that the higher rate of aggregation for pA $\beta$  is predominantly caused by a more efficient nucleation, during which a higher number of small aggregates are formed. To prove increased oligomer formation of pA $\beta$ , samples were separated by SDS-PAGE and A $\beta$  variants detected by western blotting (WB). As compared with npA $\beta$ , pA $\beta$  formed SDS-resistant low-molecular weight oligomers (i.e. dimers and trimers) much faster (Figure 2C). Consistent with faster nucleation and oligomer formation, pA $\beta$  also showed increased aggregation into larger assemblies that were detected as smears at the upper parts of the gels. These data demonstrate that phosphorylation of A $\beta$  strongly promotes the formation of low-molecular weight oligomers and further aggregation into fibrils.

The formation of small soluble oligomers is associated with conformational changes resulting in increased  $\beta$ -sheet structure. We first measured the structural conversion of A $\beta$  monomers to aggregates by circular dichroism (CD) spectroscopy. At the start of the aggregation assay, the initial far-UV CD spectrum of npA $\beta$  revealed the characteristic features of a mostly random coil state (Figure 2D). Incubation of npA $\beta$  at 37°C resulted in a prominent change in the CD spectrum. After incubation for 8 h, a CD profile was observed that is characteristic for extended  $\beta$ -sheet structure (broad negative peak at 210–220 nm; Figure 2D). The initial CD spectrum of pA $\beta$  was also as expected for an unfolded peptide. However, a characteristic pattern of extended  $\beta$ -sheet structure was clearly evident already after 2 h of incubation (Figure 2E), indicating that phosphorylation increases the propensity of A $\beta$  to adopt a  $\beta$ -sheet conformation and thereby promotes oligomerization. The combined *in vitro* data demonstrate that phosphorylation of A $\beta$  at Ser8 promotes the formation of oligomers that could increase aggregation.

Next, we compared the effect of pA $\beta$  and npA $\beta$  variants in nucleation-dependent polymerization. As expected, pre-formed oligomeric nuclei of npA $\beta$  significantly reduced the lag period of fibril formation as compared with a non-seeded reaction (Figure 2F). More interestingly, oligomeric nuclei of

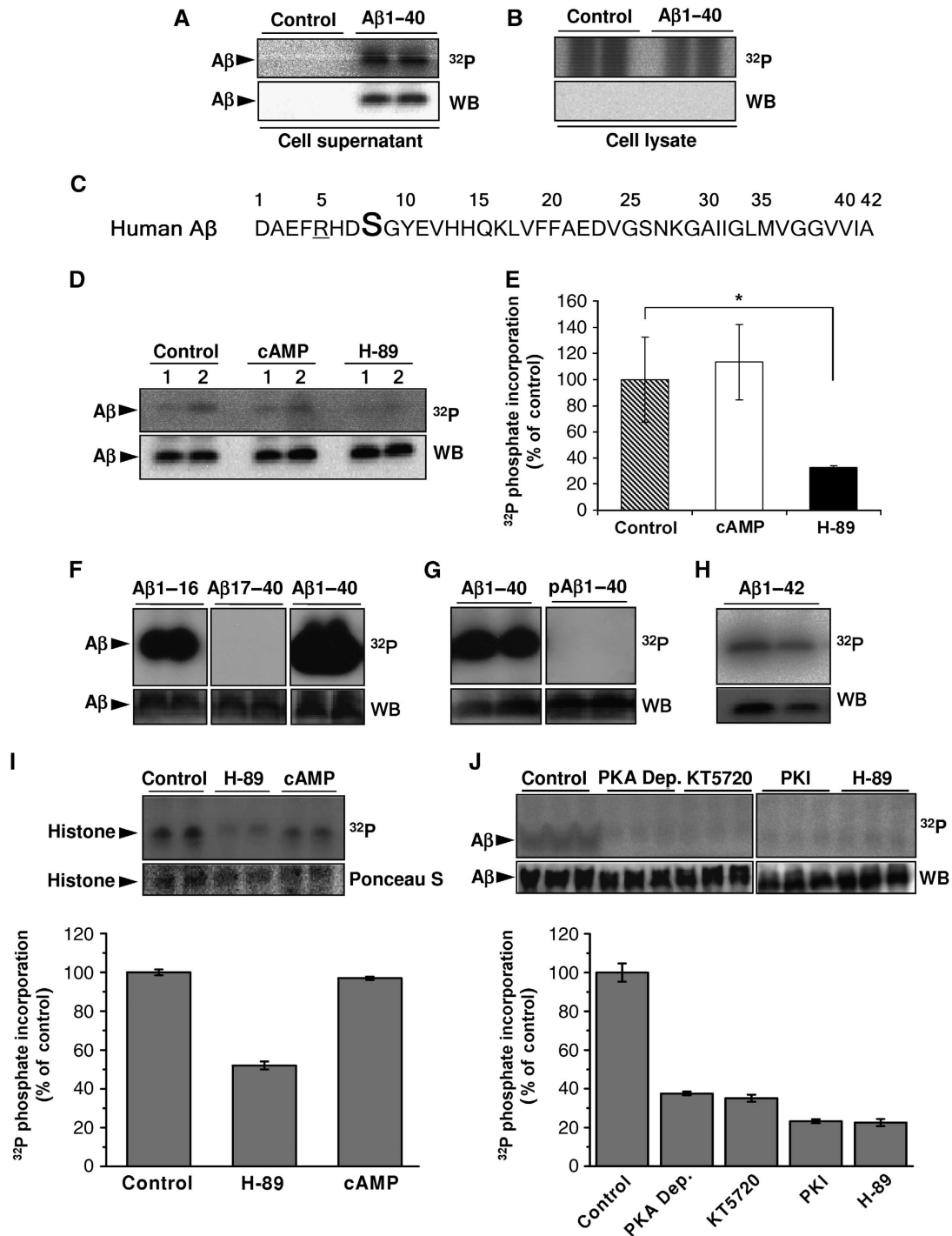


**Figure 1** Phosphorylation of A $\beta$  at Ser8. (A, B) Primary cultures of mouse cortical neurons were incubated with 10  $\mu$ M [ $\gamma$ - $^{32}$ P]ATP in the presence or absence of synthetic A $\beta$ 1-40 for 30 min at 37°C. After incubation, A $\beta$  was immunoprecipitated from cell supernatants (A) and cell lysates (B) and was separated by SDS-PAGE, transferred onto nitrocellulose membranes and detected by autoradiography ( $^{32}$ P) and WB. (C) Amino-acid sequence of human A $\beta$  in single letter code. Ser8 (bold) and arginine residue 5 (underlined) resemble a consensus motif for PKA. (D, E) Phosphorylation of A $\beta$ 1-40 by primary mouse cortical neurons (1, 1  $\times$  10<sup>6</sup> cells; 2, 2  $\times$  10<sup>6</sup> cells) in the absence or presence of 2.5  $\mu$ M cAMP or 1  $\mu$ M H-89 were performed as described above and quantified by phospho-imaging (E).  $^{32}$ P-values represent means  $\pm$  s.d. ( $n = 3$ ). Statistical significance was evaluated by paired *t*-test ( $^*P < 0.05$ ). (F-H) *In vitro* phosphorylation of A $\beta$  variants by purified PKA. Synthetic peptides representing A $\beta$ 1-16, A $\beta$ 17-40, A $\beta$ 1-40 (F), A $\beta$ 1-40 phosphorylated at Ser8 (pA $\beta$ 1-40; (G)) and A $\beta$ 1-42 (H) were incubated with purified PKA and [ $\gamma$ - $^{32}$ P]ATP for 15 min at 32°C. pA $\beta$  variants were detected by autoradiography followed by WB with appropriate antibodies (A $\beta$ 1-16, A $\beta$ 1-40, A $\beta$ 1-42, pA $\beta$ 1-40 with antibody 82E1; A $\beta$ 17-40 with antibody 4G8). (I, J) *Ex vivo* phosphorylation in human CSF. Human CSF was incubated with 10  $\mu$ M [ $\gamma$ - $^{32}$ P]ATP together with histone (I) or A $\beta$ 1-40 (J) in the absence or presence of the indicated kinase inhibitors (H-89, PKI and KT5720) or cAMP. PKA Dep., CSF after immunodepletion of PKA with specific antibodies. The phosphate incorporation was detected by autoradiography ( $^{32}$ P) and quantified by phospho-imaging. Phosphorylation of A $\beta$  was also detected with lower concentrations of ATP (1.0 and 0.1  $\mu$ M; data not shown). Histone and A $\beta$  was visualized by staining with Ponceau S and WB, respectively. Values represent means  $\pm$  s.d. of three independent experiments.

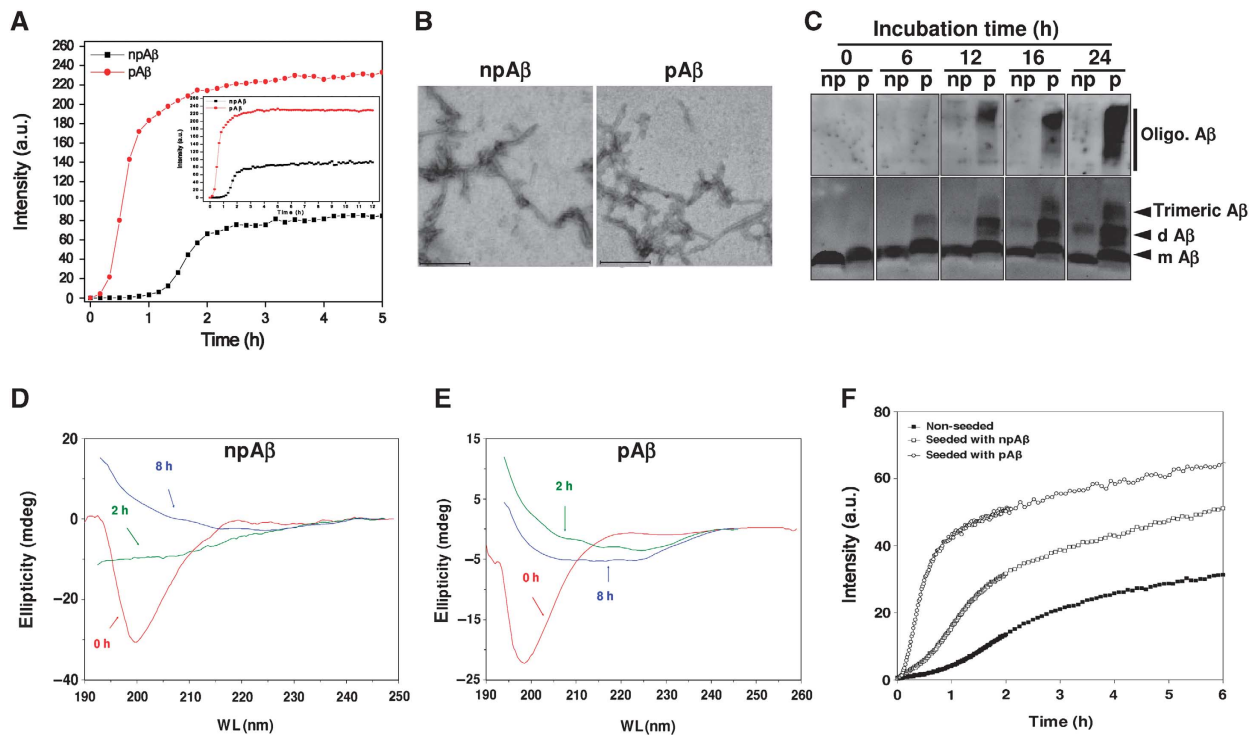


**Figure 2** Phosphorylation at Ser8 enhances aggregation of A $\beta$  by promotion of  $\beta$ -sheet conformation. (A) Aggregation of npA $\beta$ 1-40 and pA $\beta$ 1-40 was monitored by Thioflavin T (ThT) fluorescence assay. Inset image shows the measurements over 12 hours. (B) Electron micrographs of aggregates of npA $\beta$  and pA $\beta$  after 24 h. Fibrils were formed by both peptide variants and show highly similar structures. Scale bar represents 200 nm. (C) Detection of npA $\beta$  and pA $\beta$  aggregates by WB. Aliquots of the reaction mixtures from the Congo Red (CR) aggregation assay (Supplementary Figure S2) were taken at the indicated time points, separated by SDS-PAGE and A $\beta$  variants were detected with monoclonal antibody 82E1. Detection of monomeric A $\beta$ , dimeric A $\beta$ , trimeric A $\beta$  and higher oligomeric A $\beta$  forms are indicated. (D, E) Far-UV CD spectra of npA $\beta$  (D) and pA $\beta$  (E) at three different time points (0, 2 and 8 h). Phosphorylation increases the propensity of A $\beta$  to adopt a  $\beta$ -sheet conformation. (F) *In vitro* seeding of npA $\beta$  with pre-formed npA $\beta$  and pA $\beta$  aggregates was monitored by ThT fluorescence assay. Increased aggregation of npA $\beta$  can be observed with pA $\beta$  seeds as compared with npA $\beta$  seeds.

pA $\beta$  were much more efficient in promoting the aggregation reaction of npA $\beta$  and almost completely eliminated the lag phase. These data demonstrate that oligomeric nuclei of pA $\beta$  could efficiently seed the aggregation of npA $\beta$ .

#### Detection of pA $\beta$ in APP transgenic mice and human AD brain

To assess the phosphorylation of A $\beta$  and its effect on aggregation *in vivo*, we first generated phosphorylation-state-specific antibodies. Affinity purified antibody SA5434 was found to be highly specific for A $\beta$  phosphorylated at Ser8 (Supplementary Figure S3A). We also tested several monoclonal antibodies for their binding to pA $\beta$  and npA $\beta$ . While antibody 82E1 detected both peptides, the antibody 6E10 was found to be highly specific for npA $\beta$  (Supplementary Figure S3A). This antibody recognizes an epitope between amino acids 4 and 12 of the A $\beta$  domain that contains the identified phosphorylation site (Kim *et al*, 1988). Notably, SA5434 did not react with full-length APP or its C-terminal fragment in brain extracts of transgenic mice, suggesting selective phosphorylation of A $\beta$  (Supplementary Figure S4). SA5434 showed no reactivity with endogenous mouse APP in non-transgenic mice, further demonstrating the specificity of this antibody (Supplementary Figure S4). The antibody also did not cross-react with other modified A $\beta$  species, including synthetic A $\beta$  phosphorylated at Ser26 or pyro Glu-modified

A $\beta$  and with non-phosphorylated aggregates (Supplementary Figure S3B-D).

We took advantage of the phosphorylation-state-specific antibodies to analyse the accumulation and deposition of pA $\beta$  and npA $\beta$  variants in the brains of APP<sup>sw</sup>/PS1 $\Delta$ E9 double transgenic (*tg*) mice. At an age of 9 months, strong labelling of amyloid deposits with SA5434 was observed in the hippocampal region (Figure 3A). Most deposits also contained npA $\beta$  as indicated by the co-staining with antibody 6E10. In individual plaques, however, a more pronounced reactivity of SA5434 in the core was evident, suggesting preferential deposition of pA $\beta$ . Age-dependent analysis also revealed deposits of pA $\beta$  already in the cortex of 2-month-old (2m) mice (Figure 3B). A $\beta$  deposition strongly increased with age and a large overlap of staining with antibodies SA5434 and 6E10 was found, indicating co-deposition of pA $\beta$  together with npA $\beta$  in extracellular plaques. Again, pA $\beta$  appeared to be concentrated in the centre of individual plaques. We also detected small grain-like deposits selectively labelled by phospho-specific antibody SA5434 with little if any reactivity for 6E10 (Figure 3B). Such small deposits were not detected in non-transgenic mice (Supplementary Figure S5). Additional double staining revealed that smaller SA5434 positive deposits of pA $\beta$  were not labelled with the fluorescent Congo red analogue K114 (Crystal *et al*, 2003; LeVine, 2005). In contrast, larger deposits showed a large overlap of SA5434 and K114 labelling (Supplementary Figure S5).

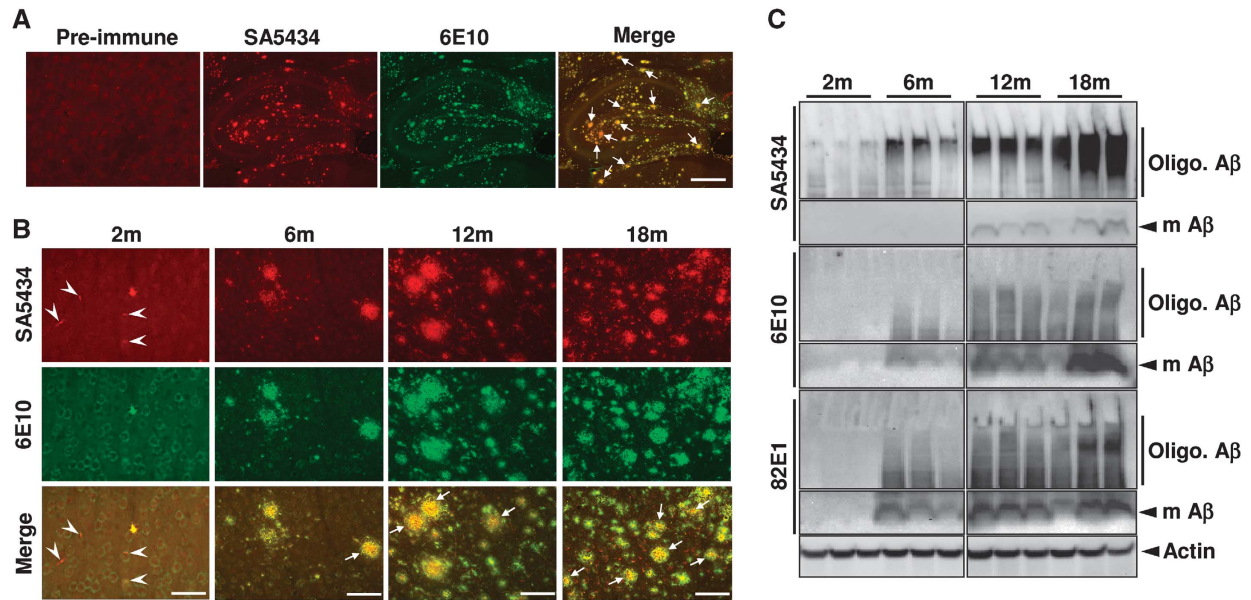


**Figure 3** Detection of pA $\beta$  in brains of APP transgenic mice. (A, B) Immunohistochemical detection of npA $\beta$  and pA $\beta$  by antibodies 6E10 and SA5434, respectively, in hippocampal regions of 9m mice (A) and in cortical regions of APPswe/PS1E9 double transgenic (*tg*) mouse brain of different ages (B). Plaques with pronounced reactivity of SA5434 in the core region are indicated by arrows. pA $\beta$  deposits selectively stained with SA5434 in 2m mice are indicated by arrowheads. The corresponding pre-immune sera (A) or SA5434 after pre-adsorption (Supplementary Figure S5) showed no specific staining. Scale bars represent 500  $\mu$ m (A), 50  $\mu$ m (B: 2m) and 200  $\mu$ m (B: 6, 12 and 18m). (C) Biochemical analysis of npA $\beta$  and pA $\beta$  in mouse brain extracts. Brain homogenates of *tg* mice from 2 to 18 months (three mice for each age) were analysed by WB with antibodies SA5434, 6E10 and 82E1. Migrations of monomeric (m A $\beta$ ) and oligomeric A $\beta$  (Oligo. A $\beta$ ) variants are indicated. The pronounced reactivity of SA5434 with smear in the upper part of the gels indicates the enrichment of pA $\beta$  in oligomeric assemblies. SA5434 did not detect pA $\beta$  in brain extracts of non-*tg* mice (Supplementary Figure S4).

To further demonstrate pA $\beta$  in brains of *tg* mice, we detected pA $\beta$  and npA $\beta$  by WB. Quantitative analysis revealed that about 20–25% of extracted monomeric A $\beta$  in 18m *tg* mice is in a phosphorylated state (Supplementary Figure S6). The reactivity of monomeric A $\beta$  with antibody 6E10 markedly increased after treatment of brain homogenates with alkaline phosphatase, also indicating that about 20–30% of monomeric A $\beta$  is in a phosphorylated state *in vivo* at this age (Supplementary Figure S7). Consistent with the immunohistochemical data, levels of pA $\beta$  and npA $\beta$  strongly increased with age (Figure 3C). Importantly, SA5434 showed strong reactivity with a smear in the upper regions of the gels, most likely representing oligomeric assemblies of A $\beta$ . These species were already detected at 2 months and became prominent at 6 months. At these ages, SA5434 detected very little monomeric A $\beta$ . In contrast, monoclonal antibody 6E10 readily detected monomeric A $\beta$  already in 6-months-old mice that strongly increased with age. As compared with antibody SA5434, the reactivity of antibody 6E10 with oligomeric A $\beta$  assemblies was much weaker and mainly detected in 12- and 18-months-old animals (Figure 3C). Together, the specific detection of npA $\beta$  and pA $\beta$  in mouse brain indicates an enrichment of pA $\beta$  in oligomeric assemblies and suggests that phosphorylation increased oligomerization of A $\beta$  *in vivo*.

Deposits containing pA $\beta$  were also detected in senile plaques in human AD brain (Figure 4A; Supplementary Figure S8). Strong reactivity with SA5434 was observed in the core of neuritic plaques, while antibody 22C11 against the extracellular domain of APP selectively detected dystrophic neurites in close proximity to the amyloid core of the neuritic

plaques (Figure 4B). Importantly, immunoprecipitation of A $\beta$  variants from distinct fractions of human AD brains revealed the selective accumulation of pA $\beta$  in SDS-resistant oligomers (Figure 4C). Antibody SA5434 immunoprecipitated almost exclusively SDS stable dimers from fractions enriched in membrane-associated/intracellular A $\beta$  (TBS-TX extracts) or insoluble/fibrillar A $\beta$  (formic acid extracts), while both monomeric and dimeric pA $\beta$  were isolated from fractions enriched in soluble extracellular A $\beta$  (TBS extract). In contrast, antibody AW8 detecting both pA $\beta$  and npA $\beta$  precipitated monomeric and dimeric forms from all three fractions. These data demonstrate that pA $\beta$  is highly enriched in oligomeric assemblies of A $\beta$  in the human AD brain and support an increased aggregation of pA $\beta$  *in vivo*. The selective detection of dimeric pA $\beta$  upon extraction with formic acid also indicates a very high stability of these toxic assemblies in the human AD brain.

#### Increased accumulation and toxicity of pseudophosphorylated A $\beta$ in *Drosophila*

*Drosophila* expresses an APP-like protein, but the lack of  $\beta$ -secretase precludes generation of endogenous A $\beta$ -like peptides (Bilen and Bonini, 2005). Thus, *Drosophila* models allow to study the aggregation of exogenous A $\beta$  variants in the absence of endogenous A $\beta$  peptides. First, we tested whether the substitution of Ser8 by an aspartate residue could mimic the aggregation promoting effect of phosphorylation. Importantly, pseudophosphorylated A $\beta$  S8D showed very similar aggregation characteristics like pA $\beta$  *in vitro* and is, therefore, suitable to mimic pA $\beta$  (Supplementary Figure S9). To prevent potential effects of the mutation on

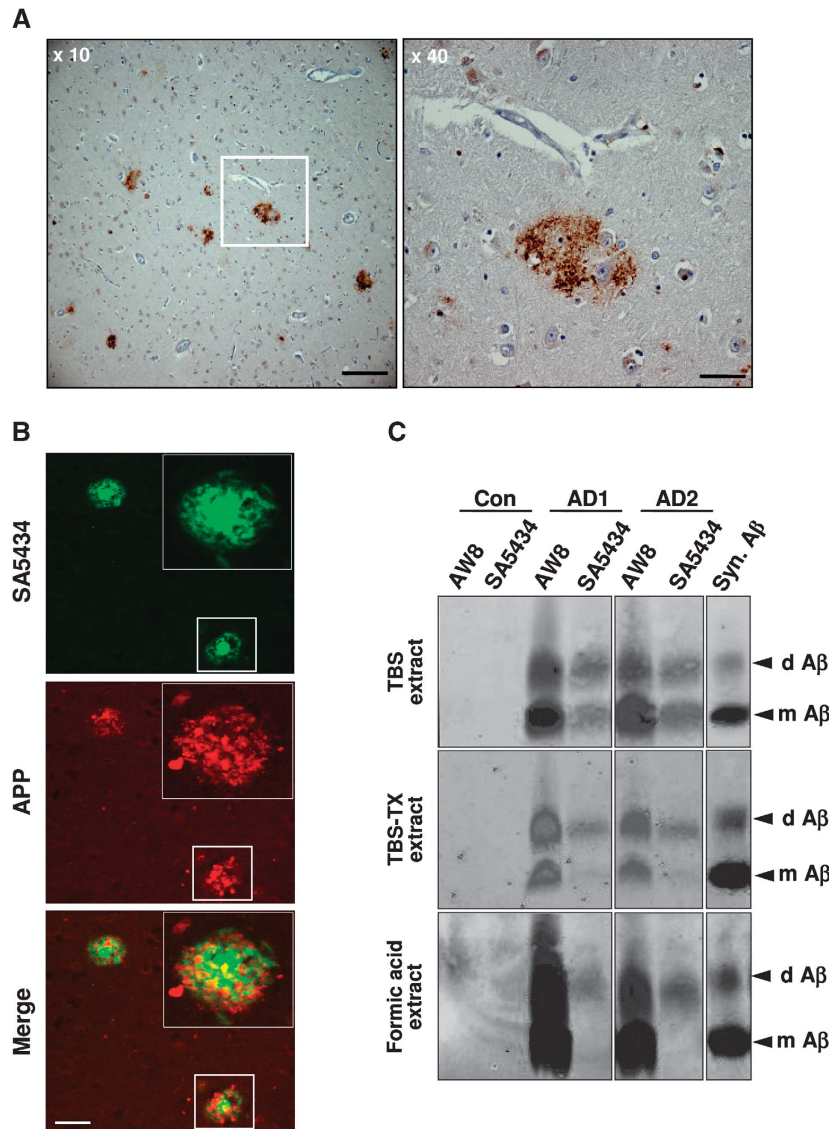


**Figure 4** Detection of pA $\beta$  in human AD brain. **(A)** Immunohistochemical staining of human AD brain with antibody SA5434. The boxed area in the left image ( $\times 10$ ) is magnified in the right panel ( $\times 40$ ). Scale bars represent  $200\ \mu\text{m}$  ( $\times 10$ ) and  $50\ \mu\text{m}$  ( $\times 40$ ), respectively. The corresponding pre-immune serum or pre-absorption of SA5434 with synthetic pA $\beta$  peptide showed no specific staining (Supplementary Figure S8). **(B)** Confocal double-label immunofluorescence photomicrographs of sections from the entorhinal cortex of a human AD brain stained with SA5434 (green) and 22C11 (red) against A $\beta$  and the APP ecto-domain, respectively. Cored neuritic pA $\beta$  plaques are associated with swollen APP-positive dystrophic neurites. Scale bar represents  $100\ \mu\text{m}$ . **(C)** Detection of pA $\beta$  in human AD brains. Brains of two AD cases (AD1 and AD2) or a control (Con.) were homogenized and sequentially extracted. Fractions enriched in extracellular soluble (TBS), membrane-associated (TBS-TX) and insoluble (formic acid) forms of A $\beta$  were immunoprecipitated with polyclonal antibodies AW8 or SA5434. A $\beta$  was then detected with monoclonal antibodies 2G3 (to A $\beta$ 40) and 21F12 (to A $\beta$ 42). Quantitative analysis by infrared imaging (as described in the Materials and methods section) revealed that about 46% in AD1 and 30% in AD2 of dimeric A $\beta$  in the TBS fraction is in a phosphorylated state.

processing, we generated constructs encoding the A $\beta$  domain with signal sequence that drives selective expression of A $\beta$  variants in the secretory pathway (Crowther *et al*, 2005). By quantitative real-time RT-PCR, we identified transgenic lines that express similar mRNA levels (Supplementary Figure S10A).

Consistent with previous results (Finelli *et al*, 2004; Crowther *et al*, 2005), expression of A $\beta$  led to age-dependent degeneration of eyes (Figure 5A). Notably, the pseudophosphorylated A $\beta$  S8D variant led to strongly increased degeneration as compared with A $\beta$  WT (Figure 5A; Supplementary Figure S10B). The degeneration of eyes was associated with

significant death of photoreceptor cells (Figure 5B), demonstrating increased toxicity of pseudophosphorylated A $\beta$ . Together, these data indicate that (pseudo)phosphorylated A $\beta$  exerts increased toxicity *in vivo*. We also detected A $\beta$  levels in corresponding eye extracts. Similar levels of A $\beta$  WT and A $\beta$  S8D were detected in extracts of 1-day-old flies, also indicating similar expression of both A $\beta$  variants (Figure 5C). Importantly, pseudophosphorylated A $\beta$  S8D accumulated to much higher levels as compared with A $\beta$  WT in 24-day-old flies (Figure 5C), strongly indicating that pseudophosphorylated A $\beta$  S8D showed increased aggregation and accumulation *in vivo*. Next, we also tested the effects of A $\beta$  WT and A $\beta$

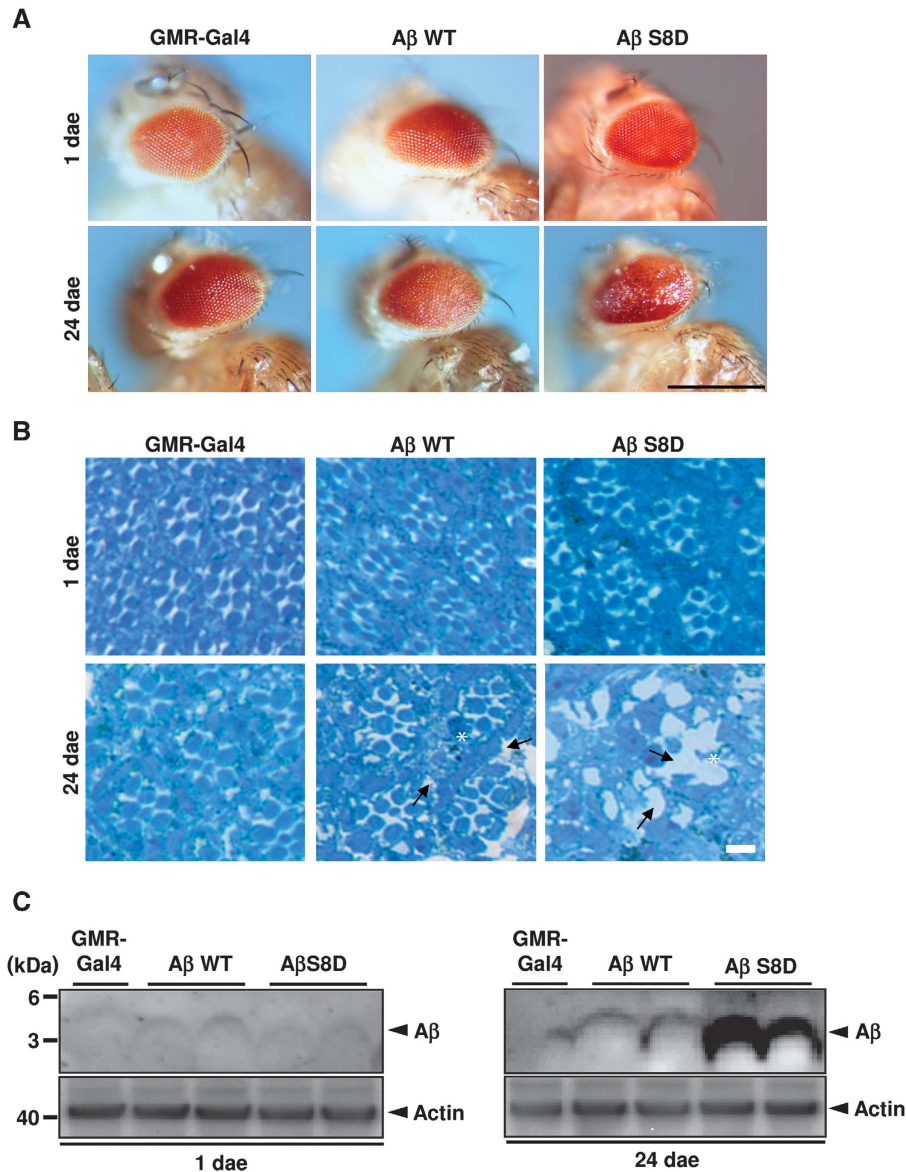


**Figure 5** Mimicking phosphorylation of A $\beta$  results in increased eye degeneration and A $\beta$  accumulation in *Drosophila*. (**A**, **B**) Transgenic *D. melanogaster* with eye-specific expression of A $\beta$  WT or A $\beta$ S8D (pseudophosphorylated) were analysed at 1st and 24th day after eclosion (dae). Flies expressing GMR-Gal4 served as control. Morphology of eyes (**A**) and cross-sections of eyes after staining with toluidine blue (**B**) was analysed by light microscopy. At first dae, eyes of control (GMR-Gal4) and A $\beta$ -expressing flies show normal morphology. Expression of A $\beta$  S8D led to increased age-dependent degeneration of eyes (**A**) and photoreceptor cells (**B**) as compared with A $\beta$ WT. A $\beta$  WT flies show missing photoreceptors (asterisk) and vacuoles in the tissue (arrows), whereas eyes of A $\beta$  S8D flies show an almost complete loss of ommatidia with occasional residual photoreceptors (asterisk) and large vacuoles (arrows). Large vacuoles in eyes of A $\beta$  S8D-expressing flies indicate increased degeneration as compared with A $\beta$  WT-expressing cells. Scale bars in (**A**, **B**) represent 0.5 mm and 50  $\mu$ m, respectively. (**C**) Western immunoblot analysis of A $\beta$  expression in eyes extracts of transgenic lines at 1st (left panel) and 24th (right panel) dae. GMR-Gal4 line served as control. Similar levels of A $\beta$  WT and S8D variants were detected at first dae (left panel). Similar expression of A $\beta$  WT and A $\beta$  S8D in the different lines was also demonstrated by quantitative real-time PCR (Supplementary Figure S10A). Pseudophosphorylated A $\beta$  S8D showed strong accumulation at 24th dae as compared with A $\beta$  WT (right panel). Western blotting revealed that A $\beta$  WT was not phosphorylated in *Drosophila* (Supplementary Figure S9B).

S8D variants upon neuron-specific expression in the brain on its accumulation as well as on the climbing behaviour of flies, two additional parameters for aggregation and A $\beta$ -mediated neurotoxicity *in vivo* (Luheshi *et al*, 2007). Confocal microscopic analysis of whole-mount brains revealed age-dependent accumulation of A $\beta$  peptides. As compared with A $\beta$  WT, A $\beta$  S8D showed highly increased accumulation (Figure 6A). Further, locomotor activity of A $\beta$  S8D flies shows an accelerated decrease compared with A $\beta$  WT or control flies during

ageing (Figure 6B; Supplementary Movie S1), indicating a progressive age-dependent phenotype, which is caused by A $\beta$  peptide accumulation.

## Discussion

Our data demonstrate that the phosphorylation of A $\beta$  increases its aggregation and toxicity. Since this post-translational modification can occur on WT A $\beta$ , these findings could

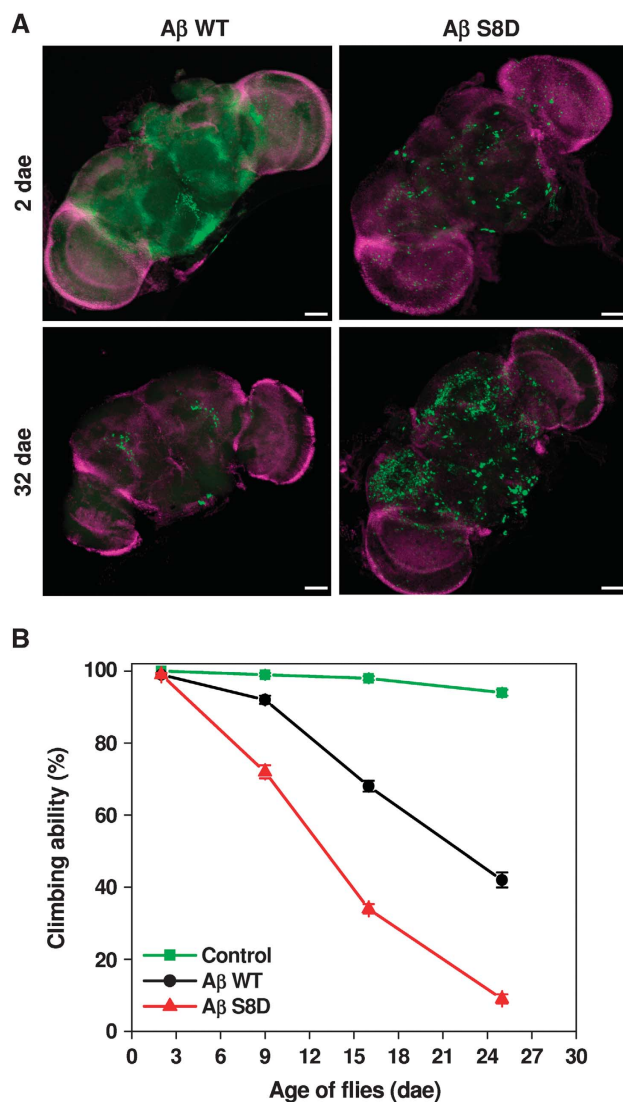


**Figure 6** Pseudophosphorylation increases A $\beta$  accumulation in the brain and induces climbing deficits. **(A)** Whole-mount immunostaining of brains from transgenic *Drosophila* expressing A $\beta$  WT or A $\beta$  S8D at dae 2 and 32 with anti-A $\beta$  antibody (green) and DAPI (magenta). Accumulation of A $\beta$  in the brain is strongly increased in flies expressing pseudophosphorylated A $\beta$  S8D as compared with those expressing A $\beta$  WT. **(B)** Analysis of age-dependent locomotor activity. As compared with control lines (elav-Gal4), flies expressing A $\beta$  WT or S8D show increased decline of climbing ability. Notably, A $\beta$  S8D induced much stronger defects as compared with A $\beta$  WT. Values represent means of five independent experiments  $\pm$  s.e.

have very important implications to the pathogenesis of sporadic, late-onset forms of AD.

Increased aggregation and formation of neurotoxic oligomers of A $\beta$  appears to be critically involved in the initiation and progression of AD (Kayed *et al*, 2003; Forman *et al*, 2004; Tsai *et al*, 2004; Spiers *et al*, 2005; Haass and Selkoe, 2007; Li *et al*, 2009). This is strongly supported by the identification of mutations within the APP and PS genes that are major causes of EOAD. These mutations commonly cause increased production of A $\beta$  variants that show an increased tendency to form toxic aggregates (Chiti *et al*, 2003). Especially, the C-terminal elongated A $\beta$ 42 shows strongly increased aggregation as compared with the A $\beta$ 40 variant. In addition, several FAD mutations are localized within or close to the

$\beta$ -turn region of A $\beta$  and could stabilize a  $\beta$ -sheet conformation of the peptide, thereby also promoting formation of neurotoxic aggregates. Recently, two mutations have been identified in the N-terminal region of A $\beta$  that also cause EOAD (Hori *et al*, 2007; Di *et al*, 2009). This is particularly interesting, because previous studies suggested that this region of the peptide is highly flexible with very little secondary structure and has a minor role in aggregation (Murakami *et al*, 2002). Moreover, a genetic mutation at position 2 of the A $\beta$  domain was recently identified to cause late-onset AD in a recessive fashion, indicating that the N-terminal part of A $\beta$  could have important roles in its aggregation and disease pathogenesis (Di *et al*, 2009). A critical role of the N-terminal domain of A $\beta$  is supported by the finding that N-terminal truncation and formation of pyroglutamate at position 3 of the A $\beta$  peptide also strongly promotes aggregation and is an abundant species found in A $\beta$  deposits in the AD brain (Saido *et al*, 1995; Schilling *et al*, 2008). It will now be interesting to assess the relative abundance of the different modified variants of A $\beta$  in human brains or CSF. Mass spectrometry would help to analyse the different modifications of A $\beta$  *in vivo* and could also provide definite proof whether they occur on individual peptides or probably in combination on the same molecule.

Protein fibrillization generally involves nucleation-dependent oligomerization as a rate-limiting step before rapid fibril growth (Rochet and Lansbury, 2000; Chiti *et al*, 2003). That A $\beta$  plaque formation could be induced by inoculation of amyloid containing brain homogenates into monkeys or APP transgenic mice suggests that nucleation-dependent fibrillization also occurs *in vivo* (Walker *et al*, 2002; Meyer-Luehmann *et al*, 2006). The rapid appearance of amyloid plaques within brains of tg mice further supports seeded growth of A $\beta$  fibrils *in vivo* (Meyer-Luehmann *et al*, 2008). Our data demonstrate that phosphorylation at Ser8 promotes the nucleation of A $\beta$  and the formation of oligomers by increasing the propensity to adopt  $\beta$ -sheet conformation. This might be caused by a relative stabilization of the more extended peptide structure in pA $\beta$ , possibly due to its higher negative charge density than the npA $\beta$ . Moreover, ordering of disordered regions in the vicinity of the site of phosphorylation might lower the entropic cost for formation of ordered aggregates, contributing to an increased aggregation in case of pA $\beta$  when compared with npA $\beta$ . Thus, phosphorylated variants of A $\beta$  could trigger oligomerization and deposition of A $\beta$  during pathogenesis of sporadic AD (Figure 7). In agreement with this hypothesis, the nuclei of pA $\beta$  were capable to promote aggregation of npA $\beta$  *in vitro* much faster than nuclei of npA $\beta$  (Figure 2F).

Importantly, the isolation of small soluble A $\beta$  assemblies from human AD brain strongly supported a critical role of pA $\beta$  species in the formation of oligomeric assemblies *in vivo*. The precipitation with antibodies specifically detecting pA $\beta$  revealed a selective enrichment in dimeric A $\beta$  variants, which are known to be highly neurotoxic (Roher *et al*, 1996; Shankar *et al*, 2008). In addition, the selective detection of pA $\beta$  in dimeric forms could also reflect increased stability of aggregates containing pA $\beta$ . Thus, it will be also interesting to assess the stability of aggregates formed by pA $\beta$  in comparison with that containing npA $\beta$ . The importance of the present finding is further supported by the detection of pA $\beta$  in neuritic plaques and SDS-stable dimers, which strongly

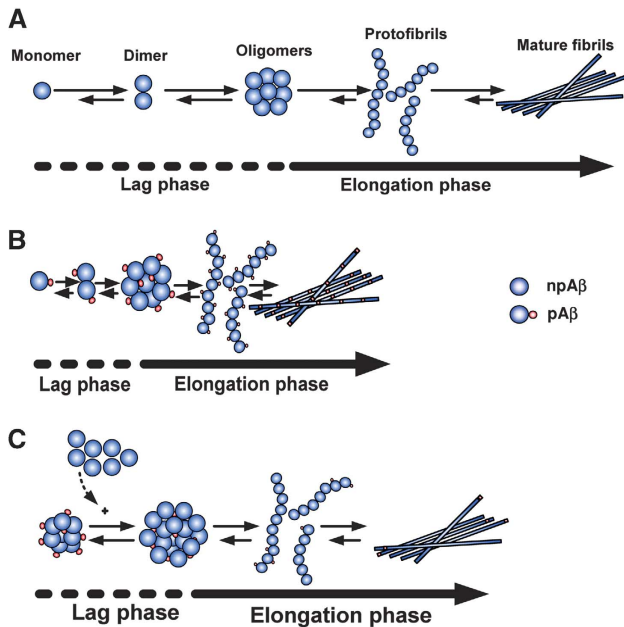


**Figure 7** Schematic diagram showing the aggregation characteristics of npA $\beta$  and pA $\beta$ . (A) Aggregation of A $\beta$  has two kinetic phases. In the 'lag phase', oligomeric nuclei are formed in a slow process (dashed lines). In the 'elongation phase', oligomeric nuclei promote fibril formation (straight line). (B) Phosphorylation of A $\beta$  reduces the lag phase of nucleation as compared with that of npA $\beta$ . (C) Nuclei of pA $\beta$  could serve as seeds to promote accelerated aggregation of npA $\beta$ .

argues in favour of a critical role of pA $\beta$  in AD-related neurodegeneration (Roher *et al*, 1996; Shankar *et al*, 2008). Furthermore, pA $\beta$  also occurs in senile plaques of *tg* mice and recent studies have shown that such A $\beta$  deposits induce plaque-associated neuritic degeneration (Tsai *et al*, 2004; Spires *et al*, 2005).

*Drosophila* is a valid model to study aggregation and toxicity of different A $\beta$  variants *in vivo*. *Drosophila melanogaster* has been utilized for the understanding of the molecular and cellular basis of AD pathogenesis (Bilen and Bonini, 2005). A $\beta$  expressing fly models offer the possibility of studying A $\beta$ -induced toxicity and clearance, aggregation propensity and neurodegeneration, genetic and pharmacological screening system for developing therapeutics for AD. Since *Drosophila* lacks  $\beta$ -secretase activity, this model allows to assess A $\beta$ -mediated toxicity in the absence of endogenous A $\beta$  species (Finelli *et al*, 2004; Bilen and Bonini, 2005; Crowther *et al*, 2005; Iijima *et al*, 2008). To mimic pA $\beta$ , Ser8 was substituted by an aspartate residue, a strategy that has been successfully used to study the effect of protein phosphorylation (Fluhrer *et al*, 2004). Importantly, the A $\beta$  S8D variant showed very similar aggregation characteristics like pA $\beta$  *in vitro*, demonstrating the suitability of this strategy. We generated constructs that drive expression of A $\beta$  variants in the secretory pathway without APP, thereby ruling out any effects of the artificial mutation on the production of A $\beta$  peptides by altered proteolytic processing of its precursor. Pseudophosphorylated A $\beta$  S8D strongly promoted age-dependent degeneration of eyes associated with death of photoreceptor cells as compared with A $\beta$  WT, supporting increased toxicity of pA $\beta$  *in vivo*. Moreover, the selective expression of

A $\beta$  variants in brain neurons led to accelerated age-dependent climbing deficits in flies expressing A $\beta$  S8D, also demonstrating increased toxicity of pA $\beta$  species in the brain. Although the exact mode of toxicity is unclear, the combined data demonstrate that mimicking phosphorylation of A $\beta$  strongly promotes age-dependent dysfunction of brain neurons. It will now be interesting to further dissect the underlying molecular pathways of pA $\beta$ -mediated toxicity and its pathophysiological implications in more detail.

The presence of extracellular protein kinase activities has been widely described, but their biological relevance is poorly understood (Redegeld *et al*, 1999). These kinases use extracellular ATP that is present in low nanomolar concentrations in the brain, but could increase locally to micromolar concentrations upon certain stimuli, including synaptic activity, inflammation and ischaemia *in vivo* (Melani *et al*, 2005; Gourine *et al*, 2007; Pedata *et al*, 2007). Our combined data suggest that an extracellular PKA-like activity is involved in the phosphorylation of A $\beta$ . Interestingly, secretion of PKA has been demonstrated with different peripheral cell types (Cho *et al*, 2000a). We here show that a PKA-like activity is also present in the conditioned media and/or the cell surface of primary mouse cortical neurons. Moreover, we identified a PKA-like activity in human CSF. These novel data strongly indicate that secretion of PKA occurs in the human brain. However, further studies are required to identify the molecular mechanism that underlie and regulate PKA secretion in the brain.

Because our data also indicate an important role of extracellular or cell surface-localized protein kinases in the pathogenesis of AD, these kinases could represent potential targets to decrease A $\beta$  aggregation and toxicity. Further, the detection of phosphorylated and npA $\beta$  in biological fluids could also be explored for evaluation as biomarkers.

## Materials and methods

### Chemicals and antibodies

The following chemicals and antibodies were used: adenosine-3', 5'-cyclic monophosphate (Biolog Life Science Institute, Germany), Congo red (AppliChem GmbH, Germany), K114, a fluorescent amyloid-specific dye (an analogue of Congo Red), Thioflavin T, Histone, H-89, PKI and KT5720 were purchased from Sigma (Germany) and A $\beta$  peptides were from Peptide Specialty Laboratory (Heidelberg, Germany). Monoclonal A $\beta$  antibodies 6E10 and 4G8 were purchased from Signet Laboratories, 82E1 antibody was from IBL Corporation (Japan), 2G3 and 21F12 antibodies, which specifically recognize A $\beta$  terminating at residues 40 and 42, were generous gift from Drs Peter Seubert and Dale Schenk (Elan Pharmaceuticals). AW8, a polyclonal anti-A $\beta$  antibody, was raised to aggregated synthetic A $\beta$ 1-42 and fluorochrome-coupled anti-mouse IR800 antibody was from Rockland (Gilbertsville, PA). Monoclonal APP antibody 22C11 was purchased from Chemicon. The Cy-2 and Cy-3 fluorochromes were from Dianova (Germany) and Alexa Fluor 488 goat anti-mouse and Alexa Fluor 594 goat anti-rabbit secondary antibodies were purchased from Invitrogen (Germany). The PKA C $\alpha$ - and C $\beta$ -specific antibodies were from Santa Cruz biotechnology.

### Generation of phosphorylation-state-specific antibodies

The polyclonal phospho-specific antibody SA5434 was generated in rabbits by inoculation of synthetic peptide that represents amino acids 1-16 of A $\beta$  with a phosphoserine at position 8 coupled to keyhole limpet haemocyanin (Eurogentec, Belgium). Phosphorylation-state-specific antibodies were isolated from the serum by double affinity purification against the phosphorylated and non-

phosphorylated peptide. The specificity of the antibodies was characterized by ELISA and WB.

#### Phosphorylation assays

*In vitro*, *in vivo* and *ex vivo* phosphorylation of A $\beta$  using purified PKA, primary mouse neurons and human CSF are described in detail in Supplementary data.

#### A $\beta$ aggregation assays

A $\beta$  aggregation assays were carried out using synthetic npA $\beta$  and pA $\beta$  peptides and monitored by Thioflavin T, Congo Red, CD Spectroscopy and transmission electron microscopy. Further information is described in Supplementary data.

#### Transgenic mice, protein extraction and immunohistochemistry

The biochemical and immunohistochemical analyses of transgenic mice were carried out using APP<sup>swE/PS1 $\Delta$ E9</sup> double transgenic mice (Strain Name: B6C3-Tg, Jax Laboratories). Preparation of brain homogenates, protein extraction, WB, quantification and immunohistochemistry are described in detail in Supplementary data.

#### Analysis of human AD brain

Human AD brains were obtained from the University Hospital Bonn with the laws and the permission of the local ethical committees. Immunofluorescence and confocal microscopy of human AD brain, human brain sample preparation and quantitation of A $\beta$  in human brain extracts by immunoprecipitation and western-blotting analysis are described in details in Supplementary data.

#### *In vitro* seeding assay

*In vitro* seeded aggregation of npA $\beta$  was carried out using preaggregated npA $\beta$  and pA $\beta$  as seeds and aggregation was

followed by ThT fluorescence measurement. The detailed procedures of all the above are described in Supplementary data.

#### Supplementary data

Supplementary data are available at *The EMBO Journal* Online (<http://www.embojournal.org>).

## Acknowledgements

We thank P Wunderlich for protein quantifications by ECL imaging, Dr C Barry for help with the *in vitro* aggregation assays, Dr D Riedel for the electron micrographs, and Dr D Crowther for providing pUAST A $\beta$ 42 and A $\beta$ 40 plasmid vectors. This work was supported by the Deutsche Forschungsgemeinschaft (DFG) to JW (WA1477/6, SFB645, KFo177) and to MZ by the DFG and the Max Planck Society.

*Author Contributions:* SK wrote parts of the paper and performed most of the experiments. DT, DRT and MTH contributed in immunohistochemical analyses and discussions; NR-G and MZ performed CD spectroscopy and seeding experiments, and contributed in data analyses and discussions. MR and MH contributed in the generation and analysis of transgenic *Drosophila*; DMW and JMM analysed pA $\beta$  in human AD brain extracts. JW conceived and supervised the research project, and wrote main parts of the manuscript. All authors were involved in the design of experiments and data interpretation.

## Conflict of interest

The authors declare that they have no conflict of interest.

## References

- Bilen J, Bonini NM (2005) *Drosophila* as a model for human neurodegenerative disease. *Annu Rev Genet* **39**: 153–171
- Chen W, Wieraszko A, Hogan MV, Yang HA, Kornecki E, Ehrlich YH (1996) Surface protein phosphorylation by ecto-protein kinase is required for the maintenance of hippocampal long-term potentiation. *Proc Natl Acad Sci USA* **93**: 8688–8693
- Chiti F, Dobson CM (2006) Protein misfolding, functional amyloid, and human disease. *Annu Rev Biochem* **75**: 333–366
- Chiti F, Stefani M, Taddei N, Ramponi G, Dobson CM (2003) Rationalization of the effects of mutations on peptide and protein aggregation rates. *Nature* **424**: 805–808
- Cho YS, Lee YN, Cho-Chung YS (2000a) Biochemical characterization of extracellular cAMP-dependent protein kinase as a tumor marker. *Biochem Biophys Res Commun* **278**: 679–684
- Cho YS, Park YG, Lee YN, Kim MK, Bates S, Tan L, Cho-Chung YS (2000b) Extracellular protein kinase A as a cancer biomarker: its expression by tumor cells and reversal by a myristate-lacking Calpha and RIIbeta subunit overexpression. *Proc Natl Acad Sci USA* **97**: 835–840
- Crowther DC, Kinghorn KJ, Miranda E, Page R, Curry JA, Duthie FA, Gubb DC, Lomas DA (2005) Intraneuronal Abeta, non-amyloid aggregates and neurodegeneration in a *Drosophila* model of Alzheimer's disease. *Neuroscience* **132**: 123–135
- Crystal AS, Giasson BI, Crowe A, Kung MP, Zhuang ZP, Trojanowski JQ, Lee VM (2003) A comparison of amyloid fibrillogenesis using the novel fluorescent compound K114. *J Neurochem* **86**: 1359–1368
- Di FG, Catania M, Morbin M, Rossi G, Suardi S, Mazzoleni G, Merlin M, Giovagnoli AR, Prioni S, Erbetta A, Falcone C, Gobbi M, Colombo L, Bastone A, Beeg M, Manzoni C, Francescucci B, Spagnoli A, Cantu L, Del FE *et al* (2009) A recessive mutation in the APP gene with dominant-negative effect on amyloidogenesis. *Science* **323**: 1473–1477
- Finelli A, Kelkar A, Song HJ, Yang H, Konsolaki M (2004) A model for studying Alzheimer's Abeta42-induced toxicity in *Drosophila melanogaster*. *Mol Cell Neurosci* **26**: 365–375
- Fuhrer R, Friedlein A, Haass C, Walter J (2004) Phosphorylation of presenilin 1 at the caspase recognition site regulates its proteolytic processing and the progression of apoptosis. *J Biol Chem* **279**: 1585–1593
- Forman MS, Trojanowski JQ, Lee VM (2004) Neurodegenerative diseases: a decade of discoveries paves the way for therapeutic breakthroughs. *Nat Med* **10**: 1055–1063
- Gourine AV, Dale N, Llaudet E, Poputnikov DM, Spyer KM, Gourine VN (2007) Release of ATP in the central nervous system during systemic inflammation: real-time measurement in the hypothalamus of conscious rabbits. *J Physiol* **585**: 305–316
- Haass C, Selkoe DJ (2007) Soluble protein oligomers in neurodegeneration: lessons from the Alzheimer's amyloid beta-peptide. *Nat Rev Mol Cell Biol* **8**: 101–112
- Harper JD, Lansbury Jr PT (1997) Models of amyloid seeding in Alzheimer's disease and scrapie: mechanistic truths and physiological consequences of the time-dependent solubility of amyloid proteins. *Annu Rev Biochem* **66**: 385–407
- Hori Y, Hashimoto T, Wakutani Y, Urakami K, Nakashima K, Condron MM, Tsubuki S, Saido TC, Teplow DB, Iwatsubo T (2007) The Tottori (D7N) and English (H6R) familial Alzheimer disease mutations accelerate Abeta fibril formation without increasing protofibril formation. *J Biol Chem* **282**: 4916–4923
- Iijima K, Chiang HC, Hearn SA, Hakker I, Gatt A, Shenton C, Granger L, Leung A, Iijima-Ando K, Zhong Y (2008) Abeta42 mutants with different aggregation profiles induce distinct pathologies in *Drosophila*. *PLoS One* **3**: e1703
- Kayed R, Head E, Thompson JL, McIntire TM, Milton SC, Cotman CW, Glabe CG (2003) Common structure of soluble amyloid oligomers implies common mechanism of pathogenesis. *Science* **300**: 486–489
- Kennedy JL, Farrer LA, Andreasen NC, Mayeux R, George-Hyslop P (2003) The genetics of adult-onset neuropsychiatric disease: complexities and conundra? *Science* **302**: 822–826
- Kim KS, Miller DL, Sapienza VJ, Chen C-M, Bai C, Grundke-Iqbal I, Currie JR, Wisniewski HM (1988) Production and characterization of monoclonal antibodies reactive to synthetic cerebrovascular amyloid peptide. *Neurosci Res Commun* **2**: 121–130

- Kirkitadze MD, Condrion MM, Teplow DB (2001) Identification and characterization of key kinetic intermediates in amyloid beta-protein fibrillogenesis. *J Mol Biol* **312**: 1103–1119
- Koffie RM, Meyer-Luehmann M, Hashimoto T, Adams KW, Mielke ML, Garcia-Alloza M, Mischeva KD, Smith SJ, Kim ML, Lee VM, Hyman BT, Spire-Jones TL (2009) Oligomeric amyloid beta associates with postsynaptic densities and correlates with excitatory synapse loss near senile plaques. *Proc Natl Acad Sci USA* **106**: 4012–4017
- Kübler D, Pyerin W, Bill O, Hotz A, Sonka J, Kinzel V (1989) Evidence for ecto-protein kinase activity that phosphorylates Kemptide in a cyclic AMP-dependent mode. *J Biol Chem* **264**: 14549–14555
- LeVine III H (2005) Mechanism of A beta(1-40) fibril-induced fluorescence of (trans,trans)-1-bromo-2,5-bis(4-hydroxystyryl)-benzene (K114). *Biochemistry* **44**: 15937–15943
- Li S, Hong S, Shepardson NE, Walsh DM, Shankar GM, Selkoe D (2009) Soluble oligomers of amyloid Beta protein facilitate hippocampal long-term depression by disrupting neuronal glutamate uptake. *Neuron* **62**: 788–801
- Luheshi LM, Tartaglia GG, Brorsson AC, Pawar AP, Watson IE, Chiti F, Vendruscolo M, Lomas DA, Dobson CM, Crowther DC (2007) Systematic *in vivo* analysis of the intrinsic determinants of amyloid Beta pathogenicity. *PLoS Biol* **5**: e290
- Mattson MP (2004) Pathways towards and away from Alzheimer's disease. *Nature* **430**: 631–639
- Melani A, Turchi D, Vannucchi MG, Cipriani S, Gianfriddo M, Pedata F (2005) ATP extracellular concentrations are increased in the rat striatum during *in vivo* ischemia. *Neurochem Int* **47**: 442–448
- Meyer-Luehmann M, Coomaraswamy J, Bolmont T, Kaeser S, Schaefer C, Kilger E, Neuenschwander A, Abramowski D, Frey P, Jaton AL, Vigouret JM, Paganetti P, Walsh DM, Mathews PM, Ghiso J, Staufenbiel M, Walker LC, Jucker M (2006) Exogenous induction of cerebral beta-amyloidogenesis is governed by agent and host. *Science* **313**: 1781–1784
- Meyer-Luehmann M, Mielke M, Spire-Jones TL, Stoothoff W, Jones P, Bacskai BJ, Hyman BT (2009) A reporter of local dendritic translocation shows plaque-related loss of neural system function in APP-transgenic mice. *J Neurosci* **29**: 12636–12640
- Meyer-Luehmann M, Spire-Jones TL, Prada C, Garcia-Alloza M, de CA, Rozkalne A, Koenigsnecht-Talboo J, Holtzman DM, Bacskai BJ, Hyman BT (2008) Rapid appearance and local toxicity of amyloid-beta plaques in a mouse model of Alzheimer's disease. *Nature* **451**: 720–724
- Murakami K, Irie K, Morimoto A, Ohigashi H, Shindo M, Nagao M, Shimizu T, Shirasawa T (2002) Synthesis, aggregation, neurotoxicity, and secondary structure of various A beta 1-42 mutants of familial Alzheimer's disease at positions 21-23. *Biochem Biophys Res Commun* **294**: 5–10
- Murakami K, Irie K, Morimoto A, Ohigashi H, Shindo M, Nagao M, Shimizu T, Shirasawa T (2003) Neurotoxicity and physicochemical properties of Abeta mutant peptides from cerebral amyloid angiopathy: implication for the pathogenesis of cerebral amyloid angiopathy and Alzheimer's disease. *J Biol Chem* **278**: 46179–46187
- Nilsberth C, Westlind-Danielsson A, Eckman CB, Condrion MM, Axelman K, Forsell C, Sten C, Luthman J, Teplow DB, Younkin SG, Naslund J, Lannfelt L (2001) The 'Arctic' APP mutation (E693G) causes Alzheimer's disease by enhanced Abeta protofibril formation. *Nat Neurosci* **4**: 887–893
- Pedata F, Melani A, Pugliese AM, Coppi E, Cipriani S, Traini C (2007) The role of ATP and adenosine in the brain under normoxic and ischemic conditions. *Purinergic Signal* **3**: 299–310
- Redegeld FA, Caldwell CC, Sitkovsky MV (1999) Ecto-protein kinases: ecto-domain phosphorylation as a novel target for pharmacological manipulation? *Trends Pharmacol Sci* **20**: 453–459
- Rochet JC, Lansbury Jr PT (2000) Amyloid fibrillogenesis: themes and variations. *Curr Opin Struct Biol* **10**: 60–68
- Roher AE, Chaney MO, Kuo YM, Webster SD, Stine WB, Haverkamp LJ, Woods AS, Cotter RJ, Tuohy JM, Krafft GA, Bonnell BS, Emmerling MR (1996) Morphology and toxicity of Abeta-(1-42) dimer derived from neuritic and vascular amyloid deposits of Alzheimer's disease. *J Biol Chem* **271**: 20631–20635
- Saido TC, Iwatsubo T, Mann DM, Shimada H, Ihara Y, Kawashima S (1995) Dominant and differential deposition of distinct beta-amyloid peptide species, A beta N3(pE), in senile plaques. *Neuron* **14**: 457–466
- Schilling S, Zeitschel U, Hoffmann T, Heiser U, Francke M, Kehlen A, Holzer M, Hutter-Paier B, Prokesch M, Windisch M, Jagla W, Schlenzig D, Lindner C, Rudolph T, Reuter G, Cynis H, Montag D, Demuth HU, Rossner S (2008) Glutaminy cyclase inhibition attenuates pyroglutamate Abeta and Alzheimer's disease-like pathology. *Nat Med* **14**: 1106–1111
- Selkoe DJ (2001) Alzheimer's disease: genes, proteins, and therapy. *Physiol Rev* **81**: 741–766
- Selkoe DJ (2008) Soluble oligomers of the amyloid beta-protein impair synaptic plasticity and behavior. *Behav Brain Res* **192**: 106–113
- Shankar GM, Li S, Mehta TH, Garcia-Munoz A, Shepardson NE, Smith I, Brett FM, Farrell MA, Rowan MJ, Lemere CA, Regan CM, Walsh DM, Sabatini BL, Selkoe DJ (2008) Amyloid-beta protein dimers isolated directly from Alzheimer's brains impair synaptic plasticity and memory. *Nat Med* **14**: 837–842
- Soto C, Estrada LD (2008) Protein misfolding and neurodegeneration. *Arch Neurol* **65**: 184–189
- Spire-Jones TL, Meyer-Luehmann M, Stern EA, McLean PJ, Skoch J, Nguyen PT, Bacskai BJ, Hyman BT (2005) Dendritic spine abnormalities in amyloid precursor protein transgenic mice demonstrated by gene transfer and intravital multiphoton microscopy. *J Neurosci* **25**: 7278–7287
- Spire-Jones TL, Meyer-Luehmann M, Osetek JD, Jones PB, Stern EA, Bacskai BJ, Hyman BT (2007) Impaired spine stability underlies plaque-related spine loss in an Alzheimer's disease mouse model. *Am J Pathol* **171**: 1304–1311
- Tanzi RE, Bertram L (2005) Twenty years of the Alzheimer's disease amyloid hypothesis: a genetic perspective. *Cell* **120**: 545–555
- Tomiyama T, Matsuyama S, Iso H, Umeda T, Takuma H, Ohnishi K, Ishibashi K, Teraoka R, Sakama N, Yamashita T, Nishitsuji K, Ito K, Shimada H, Lambert MP, Klein WL, Mori H (2010) A mouse model of amyloid {beta} oligomers: their contribution to synaptic alteration, abnormal tau phosphorylation, glial activation, and neuronal loss *in vivo*. *J Neurosci* **30**: 4845–4856
- Tsai J, Grutzendler J, Duff K, Gan WB (2004) Fibrillar amyloid deposition leads to local synaptic abnormalities and breakage of neuronal branches. *Nat Neurosci* **7**: 1181–1183
- Walker LC, Bian F, Callahan MJ, Lipinski WJ, Durham RA, LeVine H (2002) Modeling Alzheimer's disease and other proteopathies *in vivo*: is seeding the key? *Amino Acids* **23**: 87–93
- Walter J, Schnölzer M, Pyerin W, Kinzel V, Kübler D (1996) Induced release of ecto-protein kinase Yields CK-1 and CK-2 in tandem *J Biol Chem* **271**: 111–119
- Yankner BA (1996) Mechanisms of neuronal degeneration in Alzheimer's disease. *Neuron* **16**: 921–932